Digital Beam Forming Techniques for Spaceborne Reflector SAR Systems

Sigurd Huber, Marwan Younis, Anton Patyuchenko, Gerhard Krieger
Institut für Hochfrequenztechnik und Radarsysteme, Deutsches Zentrum für Luft- und Raumfahrt e.V. (DLR), Germany

Abstract

A new generation of space borne radar remote sensing systems is currently being under investigation. The concept of reflector antennas in conjunction with feed arrays, which is well established on communication satellites, is exploited for Synthetic Aperture Radar (SAR) sensors. One of the main goals for future SAR systems is to replace parts of the analog radio frequency hardware, being a major cost driver, in the receive chain with digital components. These innovative systems allow a flexible data handling and the implementation of digital beam forming (DBF) concepts. The main advantage of multi channel systems is to overcome the inherent limitations of state-of-the-art SAR instruments and enable the production of wide swath high resolution imagery at the same time. In the frame of these developments DBF algorithms, aiming at a performance improvement, are analyzed and adapted to the requirements of reflector based SAR sensors. The DBF concepts presented in this paper are illustrated by means of numerical simulations.

1 Introduction

Synthetic Aperture Radar, utilizing digital beam forming, is increasingly being considered for future earth observation missions. This is evident both from research activities [1] and space qualified technology demonstrations [2]. One of the reasons for this trend is that present-day SAR systems cannot fulfill the heterogeneous demand on products at the required performance level. The motivation for using DBF techniques is their ability to provide simultaneously a wide swath and a high resolution.
A study introducing the potential of reflector SAR systems with digital feed arrays can be found in [3]. Based on a design example in X-band, hardware optimization aspects are addressed in [4]. This paper presents digital signal processing approaches both for beam forming in elevation as well as azimuth. SAR specific performance measures like the Signal to Noise Ratio (SNR) and the Azimuth Ambiguity to Signal Ratio ($AASR$) are discussed and supplemented with numerical computations.
The reflector system consists of a parabolic reflector and a feed array of transmit/receive elements, as shown in **Figure 1**. The feed elements are arranged in the plane perpendicular to the flight direction and facing the reflector. Each element results in a beam, illuminating a region on the ground, which partially overlaps with the region illuminated by the beams of the adjacent elements. To illuminate a given angular segment in elevation, the corresponding feed elements are activated. Depending on the scan angle, one or more elements need to be activated, to avoid SNR loss. The receive beam will scan the complete swath within the time period of one PRI, whereas each element is only active during a subinterval of this time period. On transmit all N elements are activated generating a wide beam.

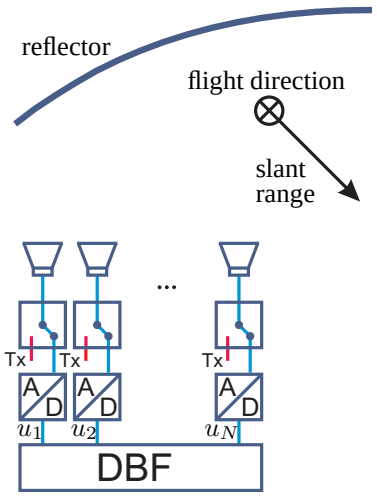

Figure 1: System architecture for reflector system; some components such as LNAs, T/R-modules, mixers, filters etc. are not shown to maintain a clear representation.

2 Digital Beam Forming Concepts

Generally the DBF concepts, considered in this paper, aim at an improvement of the system performance, namely the SNR as well as the ambiguity to signal ratio. A further issue, which is out of scope of this paper, is the effect of uncertainties on the beam forming coefficients and the implications on the performance. In the following the underlying signal model is introduced and the beam forming

approaches are explained.
The input to the digital beam former is a N-dimensional raw data vector $\mathbf{u}(t) = [u_1 u_2 ... u_N]^\top(t)$ as indicated in **Figure 1**. This signal is modeled as the received waveform $s(t)$, incorporating two way propagation and scattering, weighted with the individual complex channel pattern $\mathbf{g}(\theta) = [g_1 g_2 ... g_N]^\top(\theta)$ and superimposed by thermal receiver noise $\mathbf{n}(t) = [n_1 n_2 ... n_N]^\top(t)$ of power proportional to the receiver bandwidth.

$$\mathbf{u}(t) = \mathbf{g}(\theta)s(t) + \mathbf{n}(t) \quad . \tag{1}$$

The sampled beam-former output is a weighted linear combination of the input raw data signals

$$u_{\mathrm{DBF}}(k) = \mathbf{w}^\top(k)\mathbf{u}(k) \quad . \tag{2}$$

Assuming mutually independent signal and noise channels, the beam former output SNR can be written as

$$SNR(k) = \frac{\sigma_s^2}{\sigma_n^2} \frac{|\sum_i w_i g_i|^2}{\sum_i |w_i|^2} \quad . \tag{3}$$

Based upon equation (2) different digital beam-forming techniques are introduced in the next subsections.

3 Digital Beam Forming in Elevation

Digital beam forming in elevation denotes an operational mode, generating a wide transmit beam that illuminates the complete swath and a narrow, high gain beam on receive that follows the pulse echo on the ground [5]. Adverse to planar phased array antennas [6], in the reflector case a single activated feed element allows to illuminate a small solid angle. This means that adjacent feed element patterns do not overlap substantially. The consequence is that during the scan process different receive channels have to be switched on or off. The number of activated elements at a given time instance is dictated by the duration of the pulse and the beam widths of the single channel pattern.

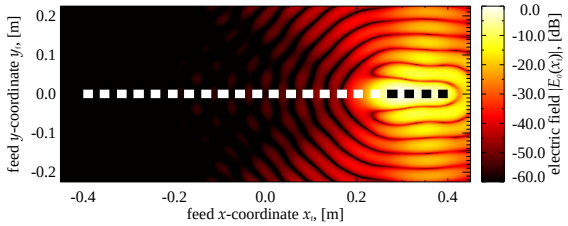

Figure 2: Normalized electric field on the feed array due to an extended pulse on the swath edge.

Looking at a certain direction θ, the corresponding channel has to be open until the signal completely has entered the system. The longer the pulse the longer the channel has to be activated. Since the echo on ground moves on, additional receive elements have to be switched on. **Figure 2** shows the field strength distribution on the feed plane due to an extended pulse in near range. The field is concentrated over a subset of feed elements, where the activated elements are represented by black patches.
In the notation of equation (2) the corresponding weight vector would look like this:

$$\mathbf{w}(k) = [0...01111]^\top \quad , \tag{4}$$

where 1 denotes an activated feed element and 0 indicates a switched off channel. Inserting equation (4) into (3) yields

$$SNR(k) = \frac{\sigma_s^2}{\sigma_n^2} \frac{1}{N_{\mathrm{act}}} \left| \sum_{i=m}^{m+N_{\mathrm{act}}-1} g_i \right|^2 \quad . \tag{5}$$

By this rudimentary beam-forming method it becomes clear, that the receive gain will drop proportional to the number of activated elements N_{act}.

3.1 Conjugate Field Matching

To overcome the large gain loss, a time varying weighting method, based on the Conjugate Field Matching (CFM) [7] principle can be applied. By this method the individual channel weights are chosen as the complex conjugate of the incident field on the feed elements.

$$\mathbf{w}(k) = \frac{\mathbf{g}^*(k)}{\mathbf{g}^\top(k)\mathbf{g}^*(k)} \quad . \tag{6}$$

In analogy to (5) the corresponding SNR is found to be

$$SNR(k) = \frac{\sigma_s^2}{\sigma_n^2} \sum_{i=m}^{m+N_{\mathrm{act}}-1} |g_i|^2 \quad . \tag{7}$$

In principle CFM allows to activate all N channels on receive simultaneously. Those channels contributing predominantly with noise are quasi nulled with small magnitude weights. Since the signals are also combined according to their phase, the high receive gain can be reconstructed at every time instance.

3.2 Frequency Adaptive Filtering

The afore mentioned principles are adequate for short pulse lengths. Consider the baseband raw data signal u_i in **Figure 3(a)** originating from two point scatterers. The selected waveform is a chirp, common for spaceborne SAR. Since both scatterers are observed under different aspect angles, they are also weighted with different feed element patterns.

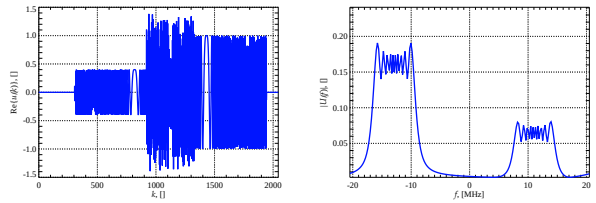

(a) raw data (b) spectral domain

Figure 3: Raw data signal u_i for two point scatterers for a single channel (left); Fourier spectrum of the raw data stream sequence for $k \in [1000, 1200]$ (right)

Consequently the weight w_i chosen for example for $k = 1000$ can only match the one signal or the other. The solution to this problem is the use of a frequency adaptive filter. Taking the Fourier transform of the overlap region between $k = 1000$ and $k = 1200$ results in two separated spectral parts. In **Figure 3(b)** the low frequency part of the large amplitude signal can be clearly distinguished from the high frequency part of the low amplitude signal. Each spectral part can now be weighted individually by means of CFM. The filter can be

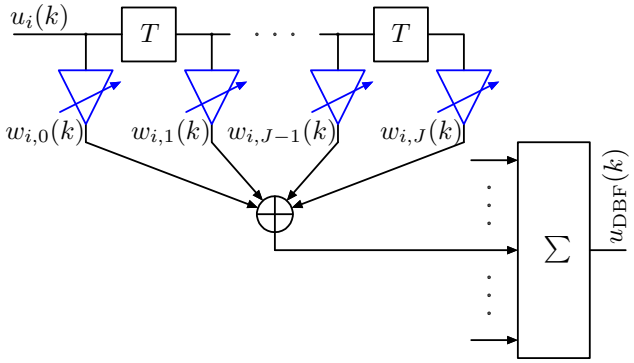

Figure 4: FIR filter with time variant coefficients.

implemented as a finite impulse response filter (FIR), as shown for the ith channel in **Figure 4**, where $J + 1$ is the total number of time variant filter coefficients $w_{i,j}(k)$ per channel and the filter order is $J = 30$. This digital beamforming approach overcomes the limitations from temporally extended pulses.

3.3 Simulations

The simulations are based on the system parameters in [4]. In the following, simulation results for four different digital beam forming algorithms are presented. The first algorithm serves as a reference, since it is independent from the pulse length and therefore performs optimal. The basic idea is to range compress the individual channel raw data streams prior to beam forming. The raw data signals of the activated channels N_{act} are than combined utilizing CFM according to equation (6). The draw back is clearly the high complexity of the digital beam former hardware and the excessive onboard processing. The second algorithm is the frequency adaptive beam former. Obviously the hardware requirements are relaxed, since FIRs with only 31 time variant coefficients are necessary in this design example. The last two algorithms are the basic unity weighting beam former (4) and the CFM algorithm (6), without any further processing.

Figure 5 shows a realization of the relative SNR over ground range.

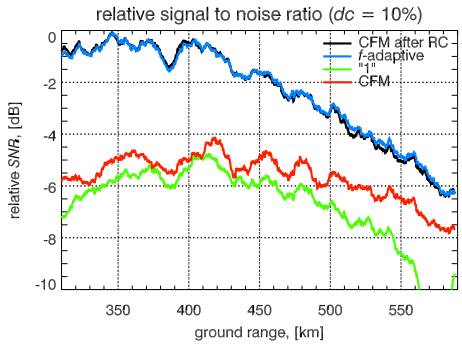

Figure 5: Relative SNR for a duty cycle of $10\,\%$.

Clearly the frequency adaptive beam former (blue curve) performs as good as the CFM based algorithm after range compression (black curve) with a drastically reduced hardware effort. CFM without further processing (red curve) suffers from weight mismatch especially in near range and the conventional channel combination approach (green curve) yields a SNR degradation proportional to the number of activated channels as indicated by equation (5).

4 Digital Beam Forming in Azimuth

By extension of the linear feed array to a two dimensional feed structure, the digital beam forming principles can also be applied to the azimuth spectrum of the SAR signal. For the following investigations a 2D-feed array with six azimuth channels, with a spacing of $0.6\,\lambda$, was chosen. Every azimuth channel is connected to an A/D converter.

The task of digital beam forming in azimuth is twofold. Firstly the optimal SNR shall be preserved and secondly the $AASR$ shall be improved at the same time for a given processed doppler bandwith B_{y}. The $AASR$ is defined according to

$$AASR = \frac{\sum\limits_{\substack{i=-\infty \\ i\neq 0}}^{\infty} \int\limits_{-B_y/2}^{B_y/2} G(f_y + iPRF)\mathrm{d}f_y}{\int\limits_{-B_y/2}^{B_y/2} G(f_y)\mathrm{d}f_y} \quad , \qquad (8)$$

where f_y is the doppler frequency, PRF is the pulse repetition frequency and $G = G_{\mathrm{Rx}}G_{\mathrm{Tx}}$ is the two way antenna gain pattern. In **Figure 6**

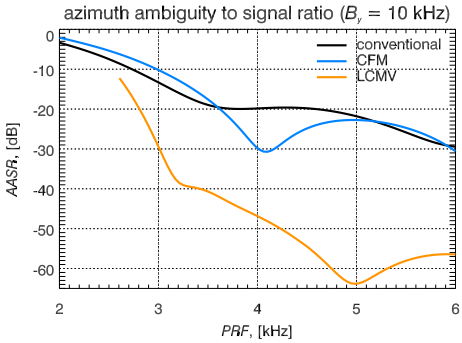

Figure 6: Azimuth ambiguity to signal ratio for the conventional case and CFM.

the $AASR$ is shown for three cases for a processed doppler bandwidth of 10 kHz. The black curve represents the conventional case, where the individual channels only contribute with a subband to the complete azimuth spectrum. This means, that overlapping spectral parts are not utilized, which results in a loss of SNR. The blue curve is generated by

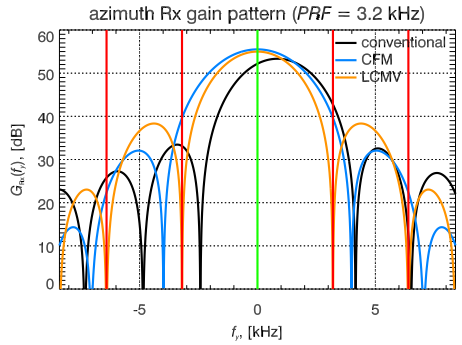

Figure 7: Azimuth gain pattern for the conventional approach, the CFM principle and the LCMV beam former

means of CFM, according to equation (6). Here all six channels are combined. The CFM based reconstruction of the azimuth spectrum outperforms the conventional case only for a small range of PRFs. A method to optimize the $AASR$ is to suppress the ambiguous directions in the receive pattern G_{Rx} in equation (8). An analytical solution for the weight vector $\mathbf{w}(f_y)$ is provided by the Linear Constraint Minimum Variance (LCMV) beam former [8]. With this approach the resulting $AASR$ is significantly improved as indicated by the orange curve.
A set of corresponding pattern is presented in **Figure 7** for a PRF of 3.2 kHz. The spectral part of interest is marked by the vertical line at doppler frequency $f_y = 0$ Hz, while the ambiguous frequencies are indicated by the red vertical lines. In the conventional case as well as in the CFM case a large part of the ambiguous signal power results from the main lobe. With the LCMV beam former the ambiguities are well suppressed at the cost of a slight SNR loss compared to the CFM principle. The LCMV beam former can also be applied in elevation in order to suppress range ambiguities.

5 Conclusion

This paper presents innovative digital beam forming concepts that allow to improve the imaging performance in terms of the Signal to Noise Ratio and ambiguity suppression. Long chirp signals, however, require more sophisticated signal processing techniques to optimize the performance. A gain loss from long chirps can be avoided by frequency adaptive filtering being realized by means of Finite Impulse Response Filters. Reflectors with digital feed arrays are therefore a promising concept for future SAR systems with high potential to outperform planar arrays.

References

[1] G. Krieger, N. Gebert, M. Younis, F. Bordoni, A. Patyuchenko, and A. Moreira, "Advanced Concepts for Ultra-Wide-Swath SAR Imaging," in *European Conference on Synthetic Aperture Radar (EUSAR)*, vol. 2, Jun 2008, pp. 31–34.

[2] C. Fischer, C. Schaefer, and C. Heer, "Technology Development for the HRWS (High Resolution Wide Swath) SAR," in *International Radar Symposium (IRS)*, Sep 2007.

[3] M. Younis, A. Patyuchenko, S. Huber, G. Krieger, and A. Moreira, "A Concept for a High Performance Reflector-Based X-Band SAR," in *European Conference on Synthetic Aperture Radar (EUSAR)*, Jun 2010.

[4] A. Patyuchenko, M. Younis, S. Huber, and G. Krieger, "Optimization Aspects of the Reflector Antenna for the Digital Beam-Forming SAR System," in *European Conference on Synthetic Aperture Radar (EUSAR)*, Jun 2010.

[5] M. Suess, B. Grafmüller, and R. Zahn, "A novel high resolution, wide swath SAR," in *IEEE International Geoscience and Remote Sensing Symposium (IGARSS)*, vol. 3, 2001, pp. 1013–1015.

[6] M. Younis, S. Huber, A. Patyuchenko, F. Bordoni, and G. Krieger, "Performance Comparison of Reflector- and Planar-Antenna based Digital Beam-Forming SAR," *International Journal of Antennas and Propagation*, vol. 2009, pp. 1–14, Jun 2009.

[7] P. T. Lam, S.-W. Lee, D. C. D. Chang, and K. Lang, "Directivity Optimization of a Reflector Antenna with Cluster Feeds: A Closed-Form Solution," *IEEE Transactions on Antennas and Propagation*, vol. 33, no. 11, pp. 1163–1174, Nov 1985.

[8] H. L. V. Trees, *Optimum Array Processing*. John Wiley & Sons, Inc., 2002.